LIQUID CRYSTALS, 1994, VOL. 17, NO. 6, 811–826

Synthesis and characterization of a semiflexible liquid crystalline polyester with a broad nematic region

by PATRICK MATHER, NINO GRIZZUTI†, GLENN HEFFNER‡, MATHIAS RICKER§, WILLIE E. ROCHEFORT‖, MARKUS SEITZ¶, HANS-WERNER SCHMIDT* and DALE S. PEARSON††

Department of Chemical and Nuclear Engineering and Materials Department, University of California, Santa Barbara, California 93106, U.S.A.

(*Received 8 February 1994; accepted 15 March 1994*)

In this paper, we report on the synthesis and detailed characterization of a new semiflexible nematic liquid crystalline polyester which could serve as a 'model' polyester for a variety of physical and physico-chemical investigations. The polymer is a nematic liquid over a wide temperature range—from the glass transition temperature at ~95°C to the isotropic transition at ~240°C. We expect this polyester to be particularly useful for studying the effect of flow on the orientation of liquid crystalline polymers, as well as the production and removal of disclinations.

1. Introduction

Interest in liquid crystalline polymers (LCPs) has undergone a rapid increase in recent years [1, 2]. The anisotropic properties of these materials make them useful for a large number of commercial products such as high strength fibres and films, directional composites, jacketing for optical cables, membranes, and precision moulded parts.

The second source of increased interest comes from the scientific community. Because flow and sometimes magnetic and electric fields are needed to process and manipulate liquid crystals, there have been extensive studies of the dynamic equations that govern their behaviour. Theoretical models, developed by a number of research groups [3–8], have made important contributions to this subject. Their work has generated a strong interest amongst experimentalists to test the predictions and to use them to develop processing methods [9–11].

† Present address: Universita di Napoli, Dipartimento di Ingegneria Chimica, Piazzale V. Tecchio, 80125, Napoli, Italia.

‡ Present address: Dupont Polymers, Experimental Station, PO Box 80101, Wilmington, DE 19880-0101.

§ Present address: Patentanwalte Strehl, Schubel-Hopf, Groening, Postfach 22 14 55, 8000 Munich, Germany.

‖ Present address: Oregon State University, Dept. of Chemical Engineering, Gleeson Hall 103, Corvallis, Oregon 97331-2702, U.S.A.

¶ Present address: Institute for Organic Chemistry, University of Mainz, 55021 Mainz, Germany.

* Author for correspondence.

†† Deceased.

0267–8292/94 $10·00

Some groups have developed experimental tools for investigating the response of macroscopically aligned LCPs to simple shear flow and flows of increasing complexity [12, 13]. Such an approach is necessary to compare closely experiment with theory. On the other hand, industrial processing methods—with the exception of fibre spinning—as applied to main chain LCPs do not yield a high degree of macroscopic alignment [14]. Instead, they lead to mottled [15] or textured [16] materials containing small regions that have a high degree of internal order but are misaligned with each other. Sometimes the regions with different orientation are arranged periodically, appearing as stripes or bands when viewed between crossed polarizers [17, 18]. Whenever any of these structures are present, it is certain that the polymer has not attained the high tensile modulus and other anisotropic properties that a full macroscopic alignment would produce.

Textured LCPs contain large quantities of orientational defects known as disclinations. Manipulation of the degree of macroscopic order in LCP products is only possible through an understanding of the creation and removal of disclinations in the presence of flow fields. As a start, our group is studying the creation of disclinations in small molecule nematics [19]. While some properties, such as high strength or ductile response, benefit from imperfection in orientation [20], it is most often desirable to eliminate defects. The possibility of mechanical property enhancement through the presence of defects has generated another need to describe the dynamics of textured materials. Recent work has suggested methods for analysing this very complicated subject [21, 22].

Rheological investigations of textured thermotropic LCPs would benefit from the ability to 'clear' the sample—change phase from nematic to isotropic—thus removing flow-induced texture and replacing it with the reproducible texture created upon cooling to the nematic phase. The low nematic–isotropic transition temperature of the material under study affords such a possibility. Primarily due to experimental convenience, most rheological and rheo-optical studies of LCPs have focused on lyotropic samples [23–30]. These materials have good optical clarity and can be studied near room temperature; however, thermal clearing for texture erasure is not possible and reproduciblity can only be achieved if samples are pre-sheared at very high rates [31]. This procedure probably does not eliminate the defects, but simply refines the texture beyond optical resolution [32]. Additionally, rheological study of lyotropic LCPs with hopes of understanding thermotropic LCP behaviour has been brought under scrutiny [33].

Commercial thermotropic liquid crystalline polymers do not have accessible clearing temperatures [34]. When they are heated toward the isotropic state, transesterification and chemical degradation intervene to change the molecular weight and structure. However, it is possible to synthesize materials with a chemical composition such that an isotropic state can be reached at temperatures far below those at which these reactions occur. Structural modifications that lower the clearing temperature have been described in several review articles [35].

In this paper we report a new semiflexible liquid crystalline polyester having a low clearing temperature. The polyester is a homopolyester which was prepared using commercially available *t*-butylhydroquinone with 4,4′-dichloroformyl-α,ω-diphenoxyhexane. The synthesis of the monomer and polymer is straightforward and can yield large quantities. Because the sample does not crystallize, it can be studied as a nematic liquid over a wide temperature range from its glass transition near 95°C to the nematic–isotropic phase transition which begins at 230°C, well below the decompo-

sition temperature. Also, complex textures can be preserved in samples quenched below the glass transition temperature for detailed study without added complications due to textural dynamics. The polymer is soluble in common solvents allowing the easy use of solution characterization techniques and, in principle, solution processing routes.

Information on the synthesis of the monomers and polymers, on molecular characterization, and on thermal studies using both calorimetry and rheometry will be discussed. Optical observations of the phase and textural behaviour are also reported. Related work on the rheological properties of liquid crystalline polymers with low clearing temperatures is reported in [36–39].

2. Experimental

2.1. *Materials*

Ethyl-4-hydroxybenzoate and 1,6-dibromohexane (Aldrich Chemical Co.) were used without further purification. *t*-Butylhydroquinone (Kodak Laboratory Chemicals) was purified by sublimation in vacuum at 100 to 110°C. A special solvent for light scattering, 3,5-bis(trifluoromethyl)phenol (BTFMP), was donated by Bayer AG, Leverkusen.

2.2. *Monomer synthesis*

The three step synthesis of 4,4′-dichloroformyl-α,ω-diphenoxyhexane (**3**) is described in the literature [40]. For completeness, and in view of slight modifications, we repeat some of the experimental details here (see figure 1). All compounds were characterized by NMR and FT-IR and gave satisfactory results.

2.2.1. *4,4′-Dicarbethoxy-α,ω-diphenoxyhexane* (**1**)

In a 250 ml one-neck flask equipped with a magnetic stir bar and a reflux condenser, 0·4 mol (66·5 g) of ethyl-4-hydroxybenzoate was dissolved in 50 ml DMF (Aldrich) to which 0·5 mol (53·0 g) of anhydrous Na_2CO_3 (Fisher Scientific) was added. Next, 0·2 mol (48·8 g) of 1,6-dibromohexane was diluted with an additional 50 ml of DMF. The mixture was refluxed with stirring for 4 h at 150°C. After cooling to room temperature, it was poured into approximately 1500 ml of water and stored in the refrigerator overnight. The precipitate was separated by filtration through a fritted glass filter (pore size C, 40–60 microns) and then washed well with water (3–4 l). Finally, the crude product was extracted in ethanol to remove residual DMF, and dried overnight at 60°C in a vacuum oven. The total amount of solid obtained was 70 g which represents a yield of 84·4 per cent. A melting point of 132°C was determined (Mel-temp II Laboratory Devices, USA) in good agreement with the literature value of 132–133·5°C [41].

2.2.2. *4,4′-Dicarboxy-α,ω-diphenoxyhexane* (**2**)

In a 1 l flask equipped with a stir bar and a reflux condenser, 0·05 mol (21·0 g) of **1** was added to 500 ml of a 10 per cent solution of KOH in ethanol. The resulting suspension was stirred and refluxed for 3 h at 120°C. After dilution with 1·5–2 l of water to dissolve the potassium salt, the suspension was heated to 50°C until a clear solution was obtained. The product was then precipitated by adding concentrated hydrochloric acid until the mixture was strongly acidic. After cooling, the solution was filtered through a fritted glass filter, the precipitate washed with water until the washing water stayed neutral to pH test paper, and then dried at 100°C *in vacuo*. The acid was separated

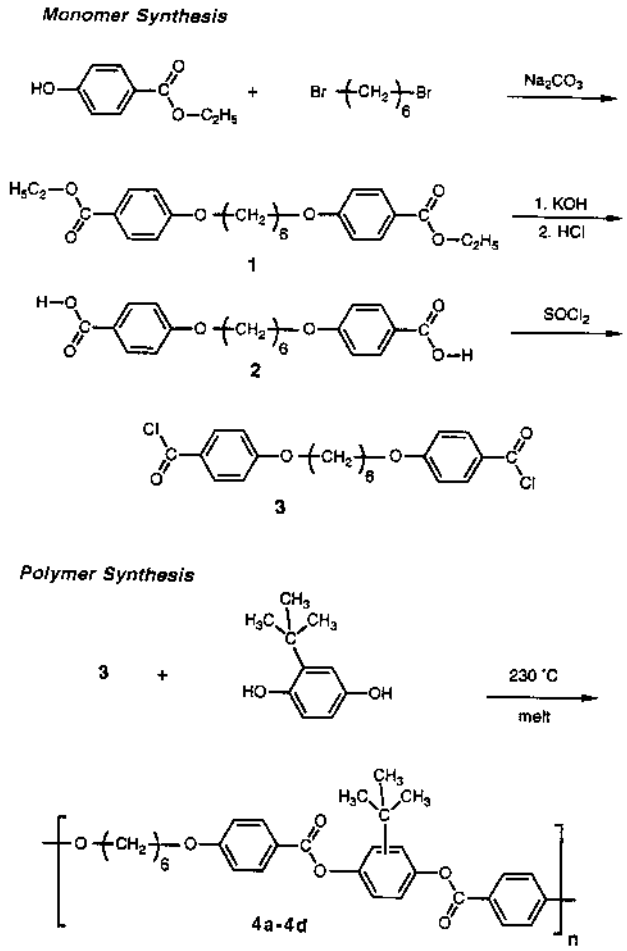

Figure 1. Synthetic route to the spacer containing monomer 4,4′-dichloroformyl-α,ω-diphenoxyhexane monomer **3** and the polycondensation reaction with *t*-butyl hydroquinone resulting in the semiflexible LC polyesters **4a–4d**.

from impurities by washing with DMF overnight in a Soxhlet extractor. A white product remained and was filtered and washed with ethanol and dried. The total amount recovered was 13·0 g which represents a yield of 72 per cent. The melting point of 290–295°C is in good agreement with the literature value of 290–292°C [40].

2.2.3. *4,4′-Dichloroformyl-α,ω-diphenoxyhexane* (**3**)

The reaction and all following operations were done under inert and dry conditions. In a 100 ml one-neck flask equipped with a reflux condenser and a stir bar, 0·06 mol (22·5 g) of **2** was refluxed for 4 h with 1·00 mol (73 ml) of thionylchloride (Fisher) and several drops of DMF as catalyst. When the reaction was completed, the excess of thionylchloride was removed by distillation at normal pressure followed by vacuum. Monomer **3** was obtained as a pale yellow solid, which was dissolved in $CHCl_3$ that had been dried over P_2O_5. The filtered solution was precipitated by slowly adding the solution into dry hexane. For 15 g of the crude **3**, about 50 ml of $CHCl_3$ are needed to dissolve it and about 300 ml of hexane for the precipitation. The precipitate was filtered

and washed well with dry hexane and dried *in vacuo*. The solid weighed 17 g (yield 70 per cent) and had a melting point of 85–88°C.

2.3. *Polymer synthesis*

Polyesters **4a** to **4d** were synthesized by a melt polycondensation of the acid chloride (**3**) and *t*-butylhydroquinone. Prior to reaction, the acid chloride was heated to its melting temperature under vacuum in order to eliminate any residual solvent which may be trapped with the crystals. The two materials were combined in stoichiometric amounts while stirring. The mixture was heated slowly to 120°C under a constant stream of argon and kept there until both components melted and a clear homogeneous melt was obtained. The evolved hydrochloric acid was removed with a stream of argon and neutralized in dilute aqueous NaOH. After a short while, formation of polymer increased the viscosity. Within the next 3–4 h, the mixture was heated to 230°C and kept at this temperature for 3–6 h. A further increase in molecular weight could be achieved by continuing the reaction under vacuum for an additional period of 1–5 h. The product was dissolved in boiling chloroform. The polymer was then precipitated by adding the $CHCl_3$ solution dropwise to a 10–15 fold excess of methanol. This dissolution and precipitation procedure was repeated once. Finally, the polymer was collected on a filter and dried under vacuum. The chemical structure of the polyesters was confirmed with FT-IR and ^1H NMR.

2.4. *Characterization procedures*

Gel permeation chromatograms in chloroform were obtained using a Spectra-Physics LC Systems GPC and Spectra 100 UV detector. The columns containing packing of pore size 10^3 and 10^5 Å (Polymer Standards Service) were calibrated with polystyrene standards of known molecular weight, and this information was used to calculate the ratio of M_w/M_n of all the samples.

The viscosity of dilute solutions of the polymers were determined in chloroform at 25°C using a Canon Ubbelohde viscometer. The intrinsic viscosity, $[\eta]$, and the Huggins coefficient, κ_H, were determined according to the following equation

$$\frac{\eta_{sp}}{c} = [\eta] + \kappa_H[\eta]^2 c, \tag{1}$$

where η_{sp} is the specific viscosity and c is the concentration. Samples were filtered through 0·5 μm PTFE filters prior to CPC and viscosity measurements.

Absolute molecular weight determinations were accomplished using a Brookhaven Instruments BI 200 SM goniometer and a Spectra Physics 15 mW helium–neon laser. Measurements on sample **4a** were made in both chloroform and in 3,5-bis(trifluoro methyl)phenol (BTFMP). The latter was recently reported to be a very good solvent for liquid crystalline polyesters [42]. Four or five concentrations of each sample were prepared by dilution of a stock polymer solution with solvent. The solutions were filtered several times through 0·5 μm filters into clean scattering cells followed by centrifugation for several hours at 5000 rpm. By examining GPC data before and after filtration, it was found that this procedure had no effect on the molecular weight distribution. Measurements were performed at 25°C. The integrated scattering intensities were recorded over the angular range of 40° to 150°. A large excess scattering at the angular extremes was observed for some concentrations, presumably due to dust remaining in the solution and flare from the cell walls. These data were neglected in the evaluation of the weight average molecular weight, M_w, and the z-average radius

of gyration, $\langle s^2\rangle_z^{1/2}$, which were determined by the usual Zimm method according to the relation [43],

$$\frac{Kc}{R_\theta} = \frac{1}{Mw}(1 + q^2\langle s^2\rangle_z/3 + 2A_2c + \ldots), \tag{2}$$

where

$$K = 4\pi n^2(dn/dc)^2/N_A\lambda_0^4$$

and

$$q = (4\pi n/\lambda_0)\sin(\theta/2).$$

R_θ is the excess Rayleigh ratio, n is the refractive, index of the solvent, λ_0 is the wavelength of light in a vacuum, N_A is Avogadros number, and dn/dc is the refractive index increment.

Refractive index increments were measured at 25°C at a wavelength of 633 nm using a C. N. Wood RF-600 differential refractometer. Values of $0{\cdot}198 \pm 0{\cdot}002$ in $CHCl_3$ and $0{\cdot}187 \pm 0{\cdot}002$ in 3,5-bis(trifluoromethyl)phenol were obtained. The concentration of solutions used for light scattering were determined by refractive index measurement and confirmed by weighing the polymer which remained after evaporation of the solvent.

Thermogravimetric analysis was performed on a Mettler TA 3000 apparatus with N_2 flush and a heating rate of 20°C min^{-1}. The samples were first dried in a vacuum oven at 100°C for 8 h. Differential scanning calorimetry data were obtained with a Perkin–Elmer DSC-7 using a heating and cooling rate of 10°C min^{-1}. Data from the second heating run are reported.

The samples were also observed using a Nikon Optiphot-Pol 104 polarizing microscope equipped with a Mettler hot stage (Model FP 82). Thin films having thicknesses of 50 to 70 μm were prepared by evaporating a solution of the polymer in chloroform at a concentration of $0{\cdot}005$ mg ml^{-1}. The films were mounted in the microscope between glass cover slides. All measurements were performed at a magnification of 100 with the polarizer and analyser axes crossed at 90°.

Dynamic oscillatory shear measurements were performed using a RMS 800 rheometer (Rheometrics, Inc.) equipped with 25 mm diameter parallel plates. Disks 1·5 mm thick and 25 mm in diameter were moulded in an evacuated cylindrical die at 230°C using powders that had been vacuum dried for 24 h at 110°C. Measurements on the samples were performed between 110°C to 270°C with a heating rate of cooling rate of 1°C min^{-1} and an angular velocity of $\omega = 1{\cdot}0$ rad s^{-1}.

3. Results and discussion

3.1. *Monomer and polymer synthesis*

A series of thermotropic polyesters, **4a,** to **4d**, differing in molecular weight were synthesized as detailed above by the melt polycondensation of acid chloride (**3**) and *t*-butylhydroquinone. The combination of these two monomers was chosen for a number of reasons. The flexible spacer in **3** is sufficiently long to lower the clearing point and to improve its solubility in organic solvents. In addition, the *t*-butyl groups on the hydroquinone are positioned randomly in a syn-or anti-configuration with respect to the following monomer unit. It is believed that this randomness adds enough irregularity to the chain to prevent crystallization or the formation of smectic phases

[35 (b)]. However, because the polyester was synthesized from one hydroquinone and one diacidchloride, transesterification reactions can not cause changes in the sequence distribution.

3.2. *Molecular characterization*

Gel permeation chromatography measurements indicate that polymers with molecular weights in excess of 10^4 have been synthesized, although the values reported in table 1 are based on polystyrene calibration. The polydispersities (M_w/M_n) of the samples are larger than 2, the value expected of polymers formed by polycondensation. The results are also similar to those reported for other unfractionated liquid crystalline polyesters [44, 45]. The GPC chromatograms were always monomodal and no low molecular weight tail was apparent (see figure 2).

The intrinsic viscosities of samples **4a–d** correspond well with the GPC-measured molecular weights and distribution, as shown in table 1. The Huggins coefficient for each sample was in the range 0·45 ± 0·05, which is typical of flexible-coil polymers in solution. This is an indication that the polymer is a true molecular solution, since aggregated molecules usually exhibit a stronger concentration dependence of the specific viscosity [46].

Light scattering experiments were performed to determine the absolute molecular

Table 1. Molecular characterization of polyesters **4a–4d** by gel permeation chromatography and dilute solution viscometry.

	GPC†			Viscometry‡
Sample	M_w	M_n	M_w/M_n	$[\eta]$, $dL\,g^{-1}$
4a	61100	25200	2·42	0·91
4b	52600	15000	3·49	0·78
4c	42300	15800	2·67	0·69
4d	13800	2500	5·55	0·32

† Polystyrene calibration.
‡ In chloroform at 25°C.

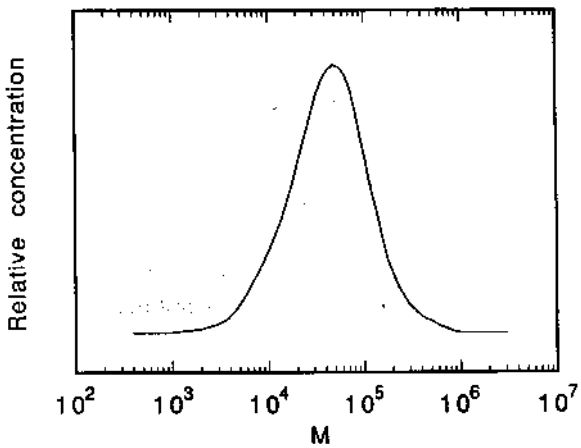

Figure 2. Gel permeation chromatogram of sample **4a**. Molecular weights on the abscissa are from polystyrene calibration.

Table 2. Molecular characteristics of polyester **4a** from light scattering at 25°C.

Solvent	M_w	$\langle s \rangle_z^{1/2}$/nm	A_2/mol × cm^3 × g^{-2}
Chloroform	34000 ± 3000	16·0 ± 2·0	$4{\cdot}1 \times 10^{-3}$
BTFMP	39000 ± 3000	16·0 ± 2·0	$5{\cdot}8 \times 10^{-3}$

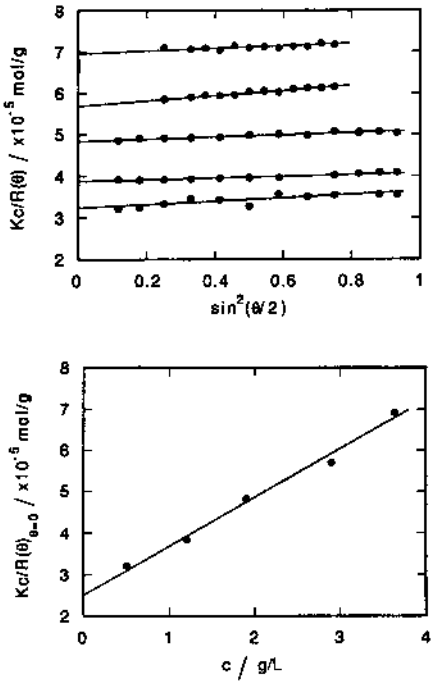

Figure 3. Light scattering data for sample **4a** in BTFMP extrapolated to zero angle (top). Extrapolation of zero angle values to zero concentration to determine M_w (bottom).

weight of sample **4a** in chloroform and in BTFMP. The same molecular weight, M_w, and radius of gyration, $\langle s^2 \rangle$, was obtained within the experimental error, regardless of the solvent used (see table 2). This fact and the positive values of the second virial coefficient, A_2, is a further indication that molecular solutions are formed in both solvents. This weight-average molecular weight corresponds to a degree of polymerization of about 70, which is in the range typical of polymers synthesized by melt polycondensation techniques. Figure 3 contains representative plots light scattering data showing the extrapolation to zero angle (top) and zero concentration (bottom).

The persistence length in solution, ρ, of the polymer was estimated using techniques appropriate for mesogenic polymers. According to the Kratky–Porod wormlike chain model [47], which may or not apply to this polymer which is nearly freely-jointed, the persistence length is related to the radius of gyration and the length of the polymer by

$$\rho = 3\langle s^2 \rangle / L \tag{3}$$

if the number of persistence lengths per macromolecular chain is large. The extended length of the polymer, L, can be calculated as $l_0 M / M_0$, where l_0 is the length of the polymer repeat unit in its most extended form, M is the polymer molecular weight, and M_0 is the monomer molecular weight. We have determined l_0 to be 2·60 nm and M_0 as

488 g mol^{-1}. Use of the weight-average molecular weight in this formula requires that the weight-average radius of gyration also be used. This was determined by adjusting the value of $\langle s^2 \rangle_z$ which we obtained from light scattering on sample **4a**, assuming a Schulz–Zimm molar mass distribution (typical of polycondensation polymers) with a polydispersity as indicated by the GPC results. The persistence length was estimated in this manner to be 2·5 ± 0·8 nm. (The error denoted here is the result of experimental uncertainties given in table 2.) The average molecule of sample **4a** is therefore equivalent to about 70 persistence lengths, which confirms that equation (2) is appropriate in this case. The fact that the persistence length is only slightly larger than the length of the mesogen (1·9 nm) indicates that the chain is quite flexible in solution due to the spacer. The observed thermotropic liquid crystalline behaviour arises from the relatively short, stiff segments along the polymer backbone. Although the chain flexibility is likely to be different in the nematic melt than in these dilute solutions, one must postulate the existence of hairpins (antiparallel mesogens linked by the spacer) in the liquid crystalline state.

3.3. *Thermal analysis and optical microscopy*

The thermal stability of sample **4a** was measured using thermogravimetric analysis. No significant weight change was observed below 380°C. Above 400°C rapid degradation is observed. Isothermal stability measurements at 260°C for more than 24 h under nitrogen on the same sample showed no weight loss due to degradation. However, slight colour changes were observed, indicating that some oxidation may have occurred.

Differential scanning calorimetry (DSC) (see table 3 and figure 4) shows that the glass transition temperatures of samples **4a** to **4d** are in the range 90–94°C. Each sample (except **4d**) also has an endothermic peak around 240°C. As confirmed by optical microscopy (see figures 6 and 7) and rheological studies (see figure 8), this peak corresponds to the nematic to isotropic transition. Even the oligomeric sample (**4d**) showed similar behaviour, although the transition temperature is lower, as expected, than the other polymers. No indication of smectic phases was found in any of the experiments. The low T_g and the weak molecular weight dependence of the clearing temperature are further indication that the flexibility is high and the liquid crystallinity is caused by the stiff mesogenic units. Table 3 gives the glass transition temperature, the nematic to isotropic transition temperature, and the enthalpy change associated with isotropization for all samples that were synthesized. The latter quantity has a value of approximately 12 J g^{-1} and is very similar to other semiflexible liquid crystalline polymers with an even number of methylene units in the backbone [48].

The texture and phase behaviour of thin films of the polymer were investigated using optical microscopy. The samples were initially conditioned, with the exception of sample **4a** photographed in figure 5, by rapidly heating them (at approximately 50°C min^{-1}) to 250°C, where the polymer is isotropic, and then cooling at the same rate to room temperature. The thermal history of the sample **4a** in figure 5 included annealing at 230°C for several hours and subsequent gradual cooling to 25°C. This annealed sample shows a very high degree of anisotropy and a complex pattern of lines (threads) generally found in nematics [49], also this sample is actually a nematic glass. This is an example of the ability to study nematic textures of this polymer under ambient conditions without the disruptive intervention of crystallization. Twist disclinations terminated by both four-brush patterns and by fuzzy patterns of two or three extinction lines can be seen. The unannealed samples were slowly heated at 1°C min^{-1} from room temperature to 250°C. Figures 6 (*a*) to (*d*) are photographs taken of a sample between

Table 3. Thermal analysis by differential scanning calorimetry (DSC) of polyesters **4a–4d**.

Sample	T_g/°C	T_{NI}/°C	ΔH_{NI}/J g^{-1}	ΔH_{NI}/kJ mol†
4a	94	245	11·6	5·7
4b	94	242	13·0	6·3
4c	90	239	12·1	5·9
4d	90	212	12·2	6·0

† kJ mol^{-1} repeat unit.

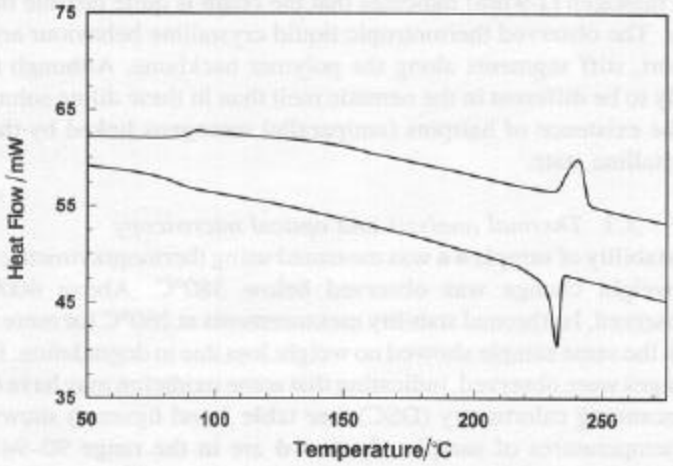

Figure 4. Differential scanning calorimetry data as a function of temperature from 50 to 265°C for sample **4a** (top curve second heating, bottom curve first cooling).

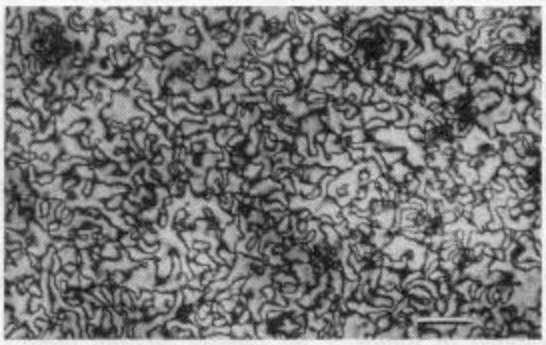

Figure 5. Photomicrograph taken of sample **4a** between crossed polarizers at 25°C. Sample was annealed at approximately 230°C for several hours prior to cooling to 25°C. Bar shown in lower right corner is 40 μm long.

crossed polarizers at 160°C, 230°C, 240°C, and 248°C, respectively. Above 100°C the material began to flow. Between 100°C and 230°C only small changes in the texture were observed and the picture taken at 160°C (see figure 6 (*a*)) is representative of the pure nematic phase which could be found up to 230°C. The transition from the pure nematic to the isotropic phase started at approximately 230°C (see figure 6 (*b*)) and coincided with the appearance of extinction regions which remained dark for all

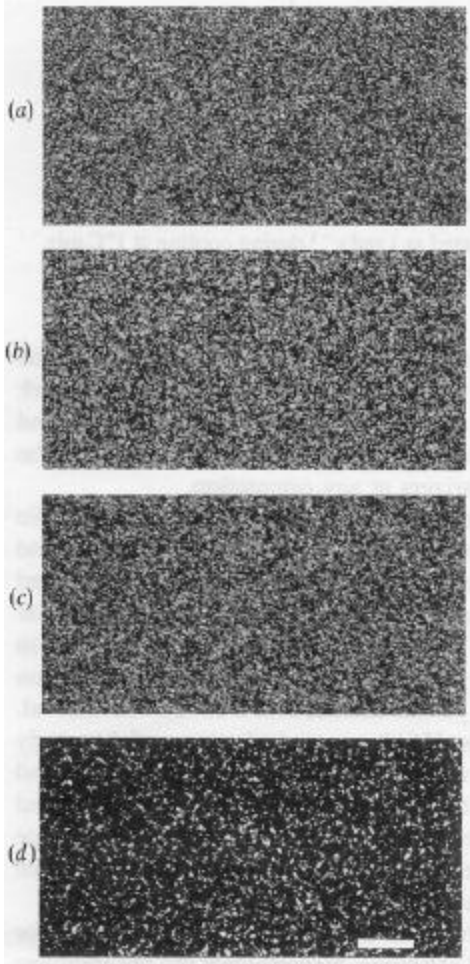

Figure 6.

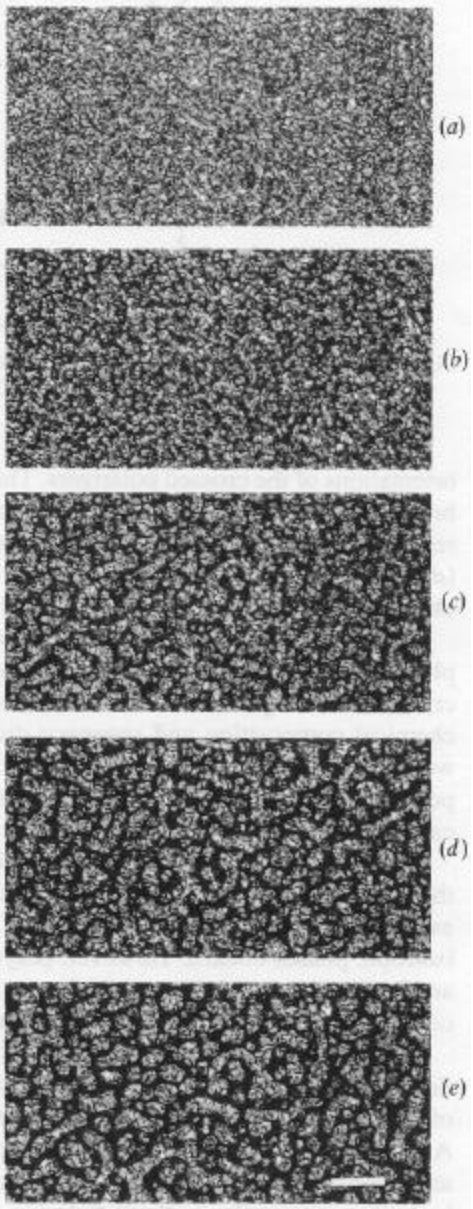

Figure 7.

Figure 6. Photomicrograph taken of a sample **4a** between crossed polarizers at 160°C (*a*), 230°C (*b*), 240°C (*c*), and 248°C (*d*). Bar shown in lower right corner is 40 μm long.

Figure 7. Photomicrographs taken every 500 s after sample **4a** initially in the one phase isotropic region at 250°C was quenched into the biphasic region at 240°C. The pictures were taken immediately after the quench (*a*), at 500 s (*b*), 1000 s (*c*), 1500 s (*d*), and 2000 s (*e*). Bar shown in lower right corner is 40 μm long.

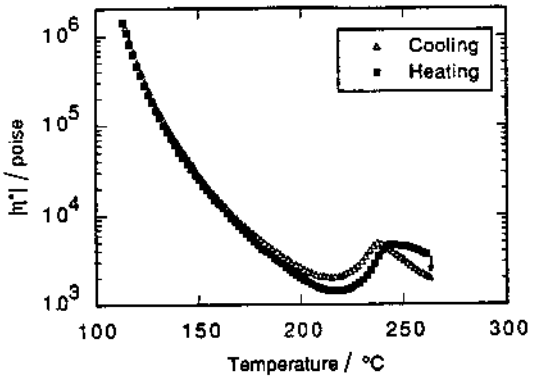

Figure 8. Dynamic viscosity of sample **4 c** measured at 1 rad s^{-1} during cooling at 1°C min^{-1} from 270°C to 110°C, then reheating to 262°C.

orientations of the crossed polarizers. This optical characteristic was different from the brush patterns which were observed to rotate with crossed polarizer rotation. The dark regions are evident in the photographs taken at 240°C and 248°C (see figure 6 (*c*) and (*d*). Above 250°C the material is fully isotropic and no transmitted light could be observed when viewed between crossed polarizers at any orientation.

The appearance of a biphasic region consisting of coexisting isotropic and nematic phases is typical for multicomponent, low molecular weight systems containing liquid crystals. Although the material we are studying is a regular copolymer with a fixed chemical composition and sequence distribution, it is polydisperse in its molecular weight. A number of other groups [50–53] have observed biphasic behaviour in polydisperse thermotropic polymers. In many cases the temperature width of the region can be quite wide. For sample for **4 a**, the two phases coexist over a 20°C wide interval.

Flory and Abe [54, 55] and Flory and Frost [56] have used a lattice model to study the effect of polydispersity on the phase diagram of solutions of rigid rods. They found as usual for lyotropic systems that there is a biphasic region in which anisotropic and isotropic phases coexist. However, polydispersity broadens the region of coexistence and leads to an enrichment of the longer molecules in the anisotropic phase the degree of which depends on the relative volume fraction of the two phases.

Theoretical descriptions of biphasic behaviour have not been as extensive for flexible polymers melts as those for rigid rod solutions. Nevertheless the observations of D'Allest *et al.* [51], on polyester melts are consistent with those of Flory [54–56]. A biphasic gap appears to be driven by the preference for the longer molecules to form an anisotropic phase. Fractionation by molecular weight is observed as well with wide biphasic gaps similar to those found in this work.

Ten Bosch, Pinton, Maissa and Sixou [57 (*a*)] have recently described a density functional method for worm-like chains with anisotropic interactions added via the Maier–Saupe potential, and the last two authors [57 (*b*)] used it to study phase diagrams of bidisperse mixtures. Semonov [58] has suggested a way of determining the width of the biphasic region that is not tied to the use of a particular interaction potential. Instead, the molecular weight dependence of the free energy of the anisotropic phase and the temperature dependence of the anisotropic and isotropic phases are used to relate the biphasic width to molecular weight and molecular weight distribution. We hope to use these ideas in future studies.

Figure 7 (*a*) to (*e*) show qualitatively the kinetics of the phase separation in the biphasic region. The micrographs were taken every 500 s after a sample initially in the one phase isotropic region at 250°C was quenched into the biphasic region at 240°C. Significant changes in the structure occur on a timescale of one hour. After about 500 s, the first nematic droplets (see figure 7 (*b*)) are observed. The volume (observed as a section area) of the regions of high anisotropy (nematic) and the dark spots (isotropic) both increased with time indicating the onset of phase separation. In agreement with earlier findings, [50, 51], nematic droplets form within the continuous isotropic phase when the sample is cooled from the isotropic melt. Without detailed analysis of the micrographs we cannot assess the time dependence, or independence, of the nematic volume fraction. Qualitatively, however, the overall brightness of the sample stayed constant during these measurements suggesting that although the size scale coarsened, the ratio of nematic to isotropic fractions remained essentially constant.

3.4. *Rheological characterization*

Dynamic oscillatory experiments were used to characterize sample **4c**. Figure 8 shows the complex viscosity, $|\eta^*(\omega = 1 \text{ rad s}^{-1})|$, as a function of temperature during a cooling and heating cycle between 110 and 260°C. Starting with a well-annealed sample in the isotropic phase at 260°C, the viscosity increases with decreasing temperature in a manner similar to all liquids. Beginning around 240°C, the viscosity begins to fall with a concomitant start of phase separation as indicated by optical microscopy. Below this temperature, the viscosity of the mixture continues to decline until approximately 220°C at which point both microscopy and calorimetry indicate that only a nematic phase is present. Below this temperature, the viscosity, as expected, begins to rise. Cooling was stopped at 110°C. This is about 15°C above the glass transition temperature and the viscosity is in excess of 10^6 Poise. On reheating, the viscosity of the nematic phase follows along the same curve recorded during cooling until the temperature is near the biphasic region. Above this temperature, the viscosity measured during heating fell below the viscosity recorded during cooling. We do not have sufficient information to explain this difference, but it is probably due to a combination of the following effects.

First, the coexisting phases not only have a difference in order but also a difference in molecular weight. Experiments [51] indicate that the nematic phase that first separates on cooling has a high molecular weight than the coexisting isotropic phase. Likewise, the isotropic phase that first separates on heating has a lower molecular weight than the coexisting ordered phase. Dissimilarity between phases in our polymers can only be due to molecular weight because the monomer sequence distribution is fixed. Variation in sequence distribution can also produce a biphasic region as has been shown by others [59].

Second, the defect concentration in the liquid crystalline phase may be different on cooling than heating. For example, the coalescence of nematic droplets during phase separation can produce disclinations [33, 60]. There are a number of mechanisms, for example pairwise annihilation of + and − defects [32, 60, 61], that could reduce the concentration of these defects during the time elapsed before the biphasic region is reached again on heating.

On further heating, it is found that the viscosity of the heating curve crosses the cooling curve and is higher by the time the isotropic phase is reached. This discrepancy must have a different explanation than the one suggested for the anisotropic phase. It cannot be due to the presence of orientational defects because they are only found in

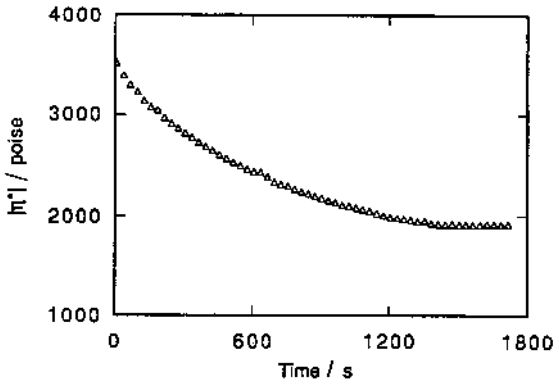

Figure 9. Relaxation of the dynamic viscosity of sample **4c** measured at 1 rad s^{-1} after the cooling–heating cycle shown in figure 8.

ordered phases. Instead, the higher viscosity is probably due to the heterogeneous mixture of high and low molecular weight materials that existed in the biphasic region and that has not had time to rehomogenize. In figure 9 we show that if the sample is held at 262°C the increased viscosity is only temporary and eventually returns to the original value of the annealed isotropic sample. The decay time constant is about 500 s. If the phase separated region have dimensions on the order of microns, a diffusion coefficient of 10^{-9} $cm^2 s^{-1}$ would be required to homogenize the sample on this time scale. Such a value seems reasonable, in light of recent measurements of tracer diffusion in semiflexible main-chain liquid crystalline polyethers [62].

4. Conclusions

A number of interesting phenomena are expected for polymers in the biphasic region, and in future studies we hope to explore them more fully. For example, the morphology in this region may not be stable but evolve with time. Flory and Frost [56] speculate that if random interchange of units can take place, such as those caused by the transesterification reactions of polyesters, then the anisotropic phase will sequester the longer molecules that are formed thus providing a mechanism for self-assembly.

We are not sure whether the patterns shown in figure 7 are due to spinoidal decomposition or nucleation and growth, but in either case, the shape of the drops should be influenced in an interesting way by the tendency for the director to align at a finite angle relative to the normal to the interface [63].

Finally, the rheological behaviour in this region and in the fully nematic region has yet to be explored. Some of the phenomena that occur during steady and oscillatory shearing should be investigated with both mechanical and optical techniques. We have recently constructed an optical rheometer that could be used to carry out such studies [64].

This work was supported by the MRL program of the National Science Foundation under Award No. DMR-9123048. One of the authors (N. G.) gratefully acknowledges support from the Consiglio Nazionale delle Richerche (Italy) in the form of a N.A.T.O. C.N.R. Fellowship.

References

[1] CIFFERRI, ALBERTO, 1991, *Liquid Crystallinity in Polymers: Principles and Fundamental Properties* (VCH Publishers, Inc.).
[2] BAHADUT, B., 1993, *Liquid, Crystals: Applications and Uses*, Vol. 1 (World Scientific).
[3] DOI, M., 1981, *J. polym. Sci. polym. Phys. Ed.*, **19,** 229.
[4] DOI, M., and EDWARDS, S. F., 1986, *The Theory of Polymer Dynamics* (Oxford University Press).
[5] SEMENOV, A. N., 1983, *Zh. eksp. teor. Fiz.*, **85,** 349.
[6] KUZUU, N., and DOI, M., 1983, *J. phys. soc. Japan*, **52,** 3486; 1984, *Ibid.*, **53,** 1031.
[7] MARRUCCI, G., and MAFFETTONE, P. L., 1989, *Macromolecules*, **22,** 4076; 1990, *J. Rheol.*, **34,** 1217.
[8] LARSON, R. G., 1990, *Macromolecules*, **23,** 3983.
[9] MOLDENAERS, P., YANASE, H., and MEWIS, J., 1991, *J. Rheol.*, **35,** 1681.
[10] LARSON, R. G., and MEAD, D. W., 1991, *J. polym. Sci. polym. Phys. Ed.*, **29,** 1271.
[11] MAGDA, J. J., BAEK, S. G., DEVRIES, K. L., and LARSON, R. G., 1991, *Macromolecules*, **22,** 4460.
[12] SRINIVASARO, M., GARAY, R. O., WINTER, H. H., and STEIN, R. S., 1992, *Molec. Crystals liq. Crystals*, **222,** 30.
[13] BURGHARDT, W. R., and FULLER, G. G., 1991, *Macromolecules*, **24,** 2546.
[14] PICKEN, S., 1990, *Macromolecules*, **23,** 3849.
[15] BERRY, G. C., 1991, *J. Rheol.*, **35,** 943.
[16] BEDFORD, S. E., and WINDLE, A. H., 1990, *Polymer*, **31,** 616.
[17] GLEESON, J. T., LARSON, R. G., MEAD, D. W., KISS, G., and CLADIS, P. E., 1992, *Liq. Crystals*, **11,** 341.
[18] PICKEN, S. J., MOLDENAERS, P., BERGHMANS, S., and MEWIS, J., 1992, *Macromolecules*, **25,** 4759.
[19] MATHER, P. T., PEARSON, D. S., and LARSON, R. G., *Liq. Crystals* (to be submitted).
[20] ZIMMER, J. E., and WHITE, J. L., 1982, *Adv. Liq. Crystals*, **5,** 157.
[21] LARSON, R. G., and DOI, M., 1991, *J. Rheol.*, **35,** 539.
[22] MARRUCCI, G., and MAFFETONE, P. L., 1990, *J. Rheol.*, **34,** 1231.
[23] MOLDENAERS, P., and MEWIS, J., 1986, *J. Rheol.*, **30,** 567.
[24] ERNST, B., NAVARD, P., HASHIMOTO, T., and TAKEBE, T., 1990, *Macromolecules*, **23,** 1370.
[25] GRIZZUTI, N., CAVELLA, S., and CICARELLE, P., 1990, *J. Rheol.*, **34,** 1293,
[26] LARSON, R. G., and MEAD, D. W., 1989, *J. Rheol.*, **28,** 504.
[27] BURGHARDT, W. R., and FULLER, G. G., 1990, *J. Rheol.*, **34,** 959.
[28] LEE, S.-D., and MEYER, R. B., 1990, *Liq. Crystals*, **17,** 15.
[29] FINCHER, C., 1986, *Macromolecules.*, **19,** 2431.
[30] ERNST, B., DENN, M. M., PERINI, P., and ROCHEFORT, W. E., 1992, *J. Rheol.*, **36,** 289.
[31] MARRUCCI, G., 1991, *Liquid Crystallinity in Polymers: Principles and Fundamental Properties*, edited by Alberto Cifferri (VCH Publishers, Inc.), Chap. 8.
[32] ERNST, B., NAVARD, P., HASHIMOTO, T., and TAKEBE, T., 1990, *Macromolecules*, **23,** 1370.
[33] BAEK, S. G., MAGDA, J. J., and LARSON, R. G., 1993, *J. Rheol.*, **37,** 1201.
[34] For example the Vectra-series polymers, manufactured by the Hoechst–Celanese Company.
[35] (a) OBER, C. K., JIN, J.-I., ZHOU, Q. F., and LENZ, R. W., 1984, *Adv. polym. Sci.*, **59,** 103; (b) SCHMIDT, H.-W., 1989, *Makromolek. Chem. Macromolek. Symp.*, **26,** 47.
[36] WISSBRUN, K. F., and GRIFFIN, A. C., 1982, *J. polym. Sci. polym. Phys. Ed.*, **20,** 1835.
[37] BLUMSTEIN, A., THOMAS, O., and KUMAR, S., 1986, *J. polym. Sci. polym. Phys. Ed.*, **24,** 27.
[38] DRISCOLL, P., FUJIWARA, K., MASUDA, T., FURUKAWA, A., and LENZ, R. W., 1988, *Polymer*, **20,** 351.
[39] KALIKA, D. S., SHEN, M.-R., YU, X.-M., DENN, M. M., IANNELLI, P., MASCIOCCHI, N., YOON, D. Y., PARRISH, W., FRIEDRICH, C., and NOËL, C., 1990, *Macromolecules*, **23,** 5192.
[40] GRIFFIN, A. C., and HAVENS, S. J., 1981, *J. polym. Sci. polym. Phys. Ed.*, **19,** 951.
[41] DONAHUE, H. B., BENJAMIN, L. E., and FENNOY, L. V., 1961, *J. org. Chem.*, **26,** 474.
[42] KRÖMER, H., KUHN, R., PIELARTZIK, H., SIEBKE, W., ECKHARDT, V., and SCHMIDT, M., 1991, *Macromolecules*, **24,** 1950.
[43] HUGLIN, M. B., 1972, *Light Scattering from Polymer Solutions* (Academic Press).
[44] LAUS, M., CARETTI, D., ANGELONI, A. S., GALLI, G., and CHIELLINI, E., 1991, *Macromolecules*, **24,** 1459.

[45] KRÖNER, H., 1991, *Macromolecules*, **24,** 1950.
[46] STICKLER, M., and SUTTERLIN, N., 1989, *Polymer Handbook*, edited by J. Brandrup and E. H. Immergut (Wiley-Interscience) Chap. 7.
[47] BRELSFORD, G. L., and KRIGBAUM, W. R., 1991, *Liquid Crystallinity in Polymers: Principles and Fundamental Properties*, edited by Alberto Cifferri (VCH Publishers, Inc.), Chap. 2.
[48] SIRIGU, A., 1991, *Liquid Crystallinity in Polymers: Principles and Fundamental Properties*, edited by Alberto Cifferri (VCH Publishers, Inc.), Chap. 7.
[49] KLEMAN, M., 1991, *Liquid Crystallinity in Polymers: Principles and Fundamental Properties*, edited by Alberto Cifferri (VCH Publishers, Inc.), Chap. 10.
[50] D'ALLEST, J. F., WU, P. P., BLUMSTEIN, A., and BLUMSTEIN, R. B., 1986, *Molec. Crystals liq. Crystals Lett.*, **3,** 103.
[51] D'ALLEST, J. F., SIXOU, P., BLUMSTEIN, A., and BLUMSTEIN, R. B., 1988, *Molec. Crystals liq. Crystals*, **157,** 229, 253, 273.
[52] D'ALLEST, J. F., TEN BOSCH, A., and SIXOU, P., 1988, *Molec. Crystals liq. Crystals, Lett.*, **6,** 15.
[53] MARTIN, P., and STUPP, S. I., 1988, *Macromolecules*, **21,** 1222.
[54] FLORY, P. J., and ABE, A., 1978, *Macromolecules*, **11,** 1119.
[55] ABE, A., and FLORY, P. J., 1978, *Macromolecules*, **11,** 1122.
[56] FLORY, P. J., and FROST, R., 1978, *Macromolecules*, **11,** 1126.
[57] (a) TEN BOSCH, A., PINTON, P. F., MAISSA, P., and SIXOU, P., 1987, *J. Phys.* A, **20,** 4531. (b) MAISSA, P., and SIXOU, P., 1989, *Liq. Crystals*, **5,** 1861.
[58] SEMENOV, A., 1993, *Europhysics Lett*, **21,** 37.
[59] STUPP, S. I., MOORE, J. S., and MARTIN, P., 1988, *Macromolecules*, **21,** 1228.
[60] CHUANG, I., TUROK, N., and YURKE, B., 1991, *Phys. Rev. Lett.*, **66,** 2472.
[61] SHIWAKU, T., NAKAI, A., SHIWAKU, T., HASEGAWA, H., and HASHIMOTO, T., 1987, *Polym. Commun.*, **24,** 174.
[62] HALL, E., OBER, C. K., KRAMER, E. J., COLBY, R. H., and GILLMOR, J. R., 1993, *Macromolecules*, **26,** 3764.
[63] DOI, M., and KUZUU, N., 1985, *J. Appl. polym. Sci. Appl. Polym. Symp.*, **41,** 65.
[64] MATHER, P., and PEARSON, D. S., *Rev. scient. Instrum.* (submitted).